

Supplementary information

Low-temperature synthesis of porous high-entropy (CoCrFeMnNi)₃O₄ spheres and their application to reverse water-gas shift reaction as catalysts

Ayano Taniguchi,^a Takeshi Fujita ^a and Kazuya Kobiro ^{*a,b}

^aGraduate School of Engineering and ^bResearch Center for Structural Nanochemistry,
Kochi University of Technology, 185 Miyanokuchi, Tosayamada, Kami, Kochi 782-8502, Japan.

*Corresponding author: kobiro.kazuya@kochi-tech.ac.jp

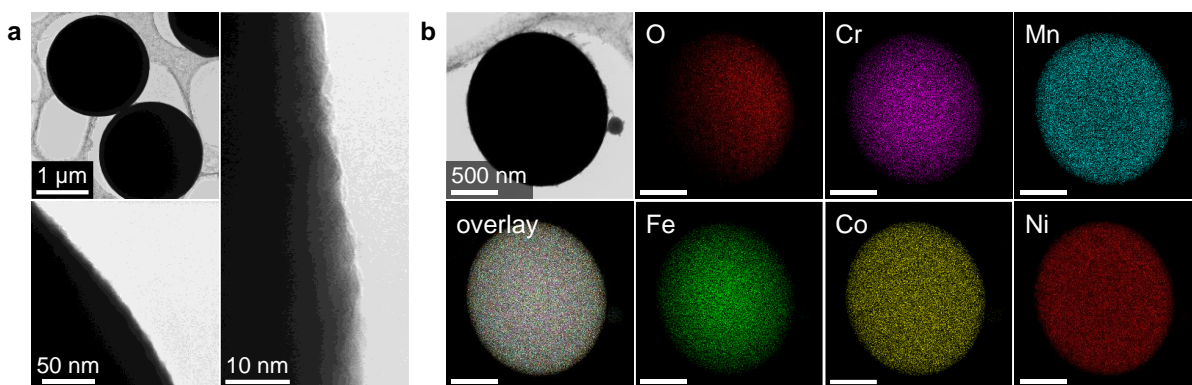


Fig. S1 TEM images (a), and STEM and EDX mapping images (b) of the precursor composite of HE-MARIMO (before calcination).

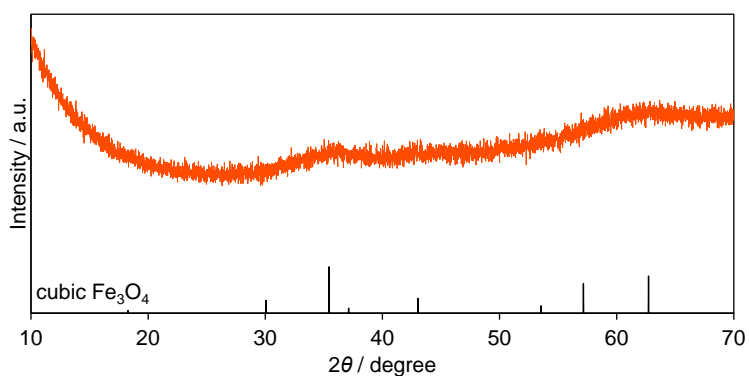


Fig. S2 XRD pattern of the precursor composite of HE-MARIMO (before calcination). The black lines correspond to reference diffraction peak positions of cubic Fe_3O_4 (PDF#00-001-1111).

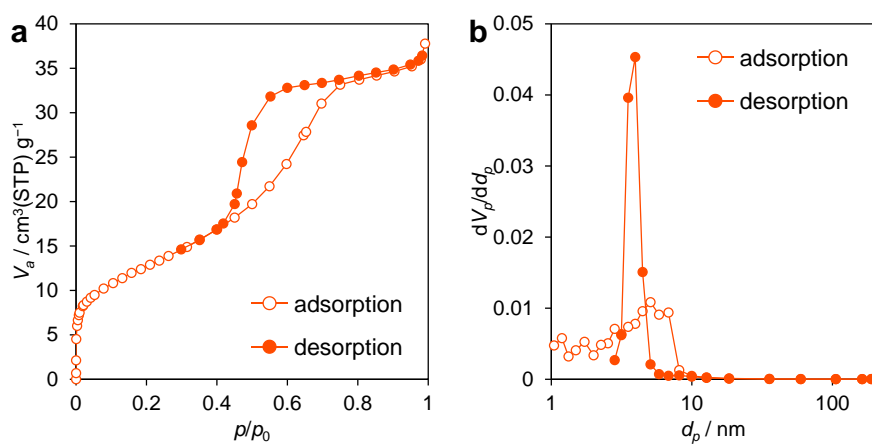


Fig. S3 Nitrogen adsorption/desorption isotherm (a) and Barrett-Joyner-Halenda plot of HE-MARIMO.

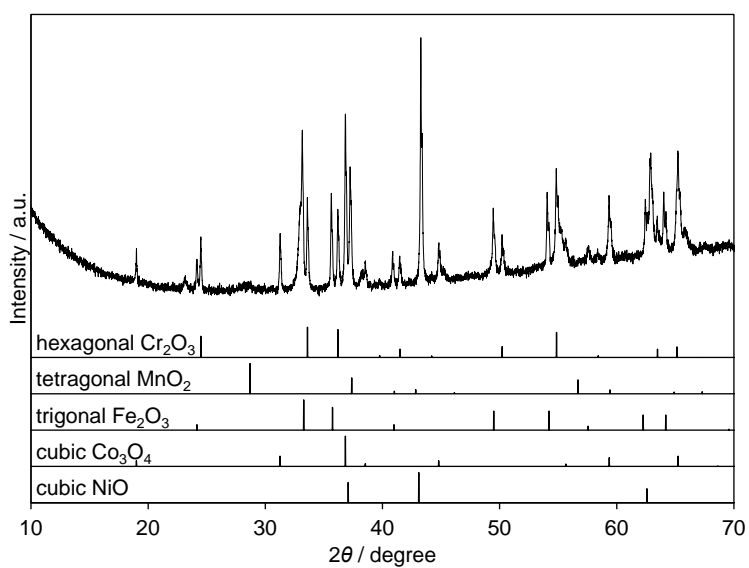


Fig. S4 XRD pattern of sss-composite. Black lines, Ref. 1, 2, 3, 4, and 5, correspond to reference diffraction peak positions of hexagonal Cr_2O_3 (PDF: 01-082-1484), tetragonal MnO_2 (PDF: 01-078-6777), trigonal Fe_2O_3 (PDF: 01-086-5601), cubic Co_3O_4 (PDF: 00-042-1467) and cubic NiO (PDF: 03-065-2901), respectively.

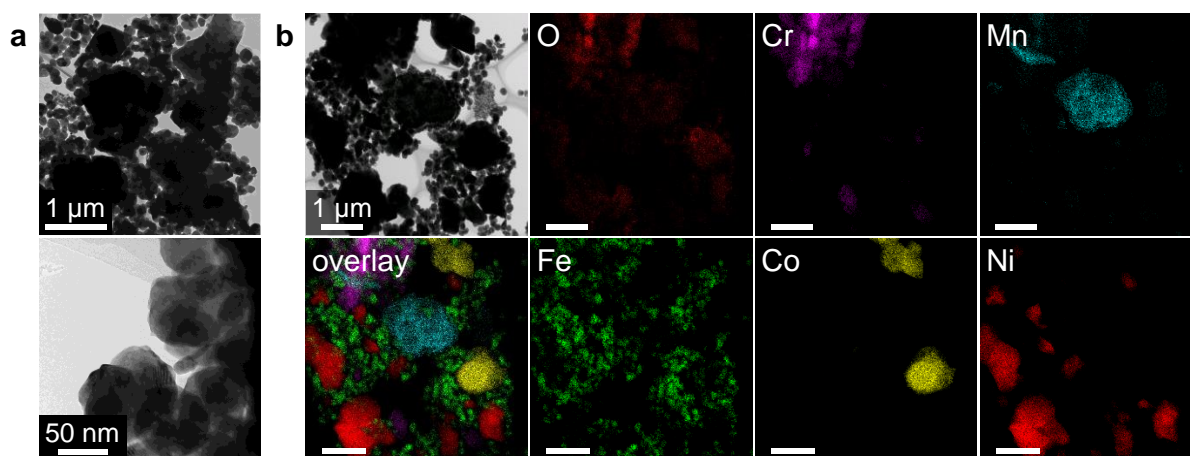


Fig. S5 TEM images (a), and STEM and EDX mapping images (b) of sss-composite.

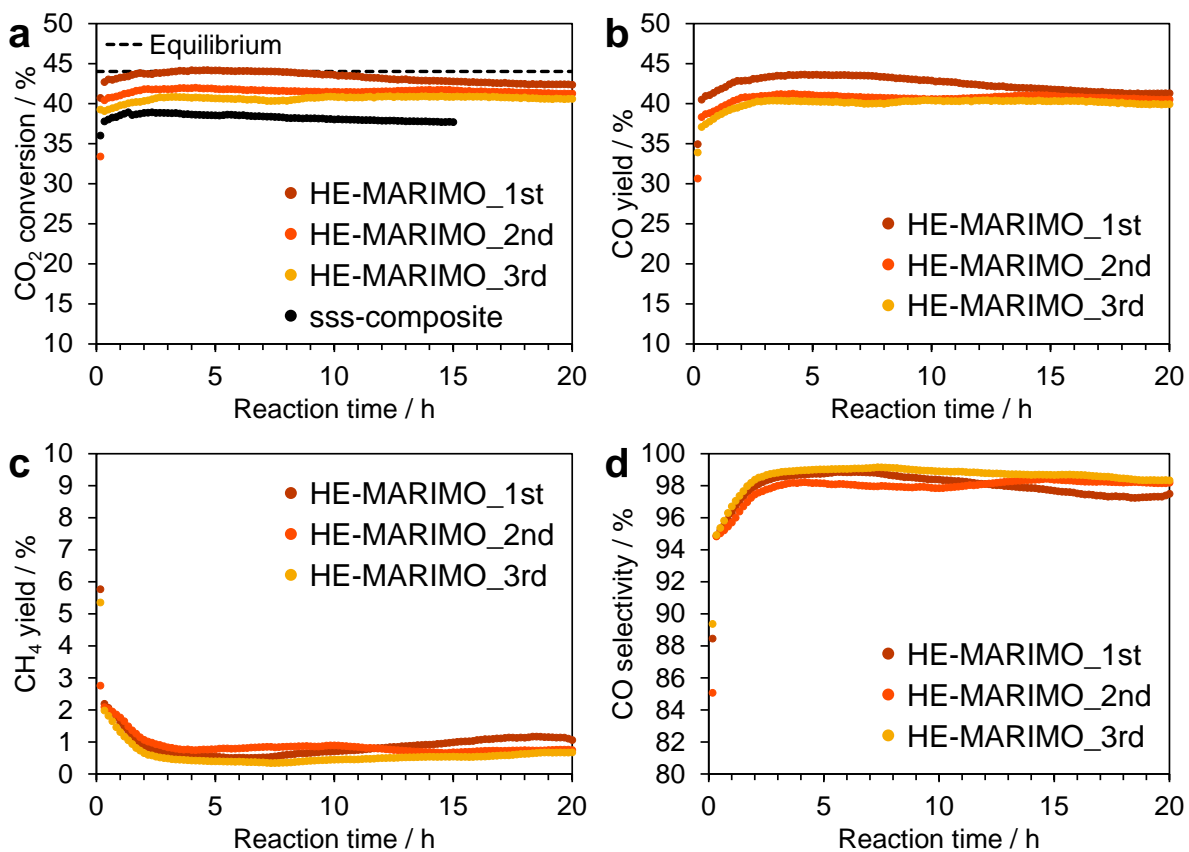


Fig. S6 Three-run cycle test for the RWGS reaction using HE-MARIMO. CO₂ conversion (a), CO yield (b), CH₄ yield (c), and CO selectivity (d) at 700 °C for 20 h (H₂/CO₂ ratio of 1:1). The CO₂ conversion result of the RWGS reaction using sss-composite [black circles in (a)] was reused for comparison. The data are the same as Fig. 4a.

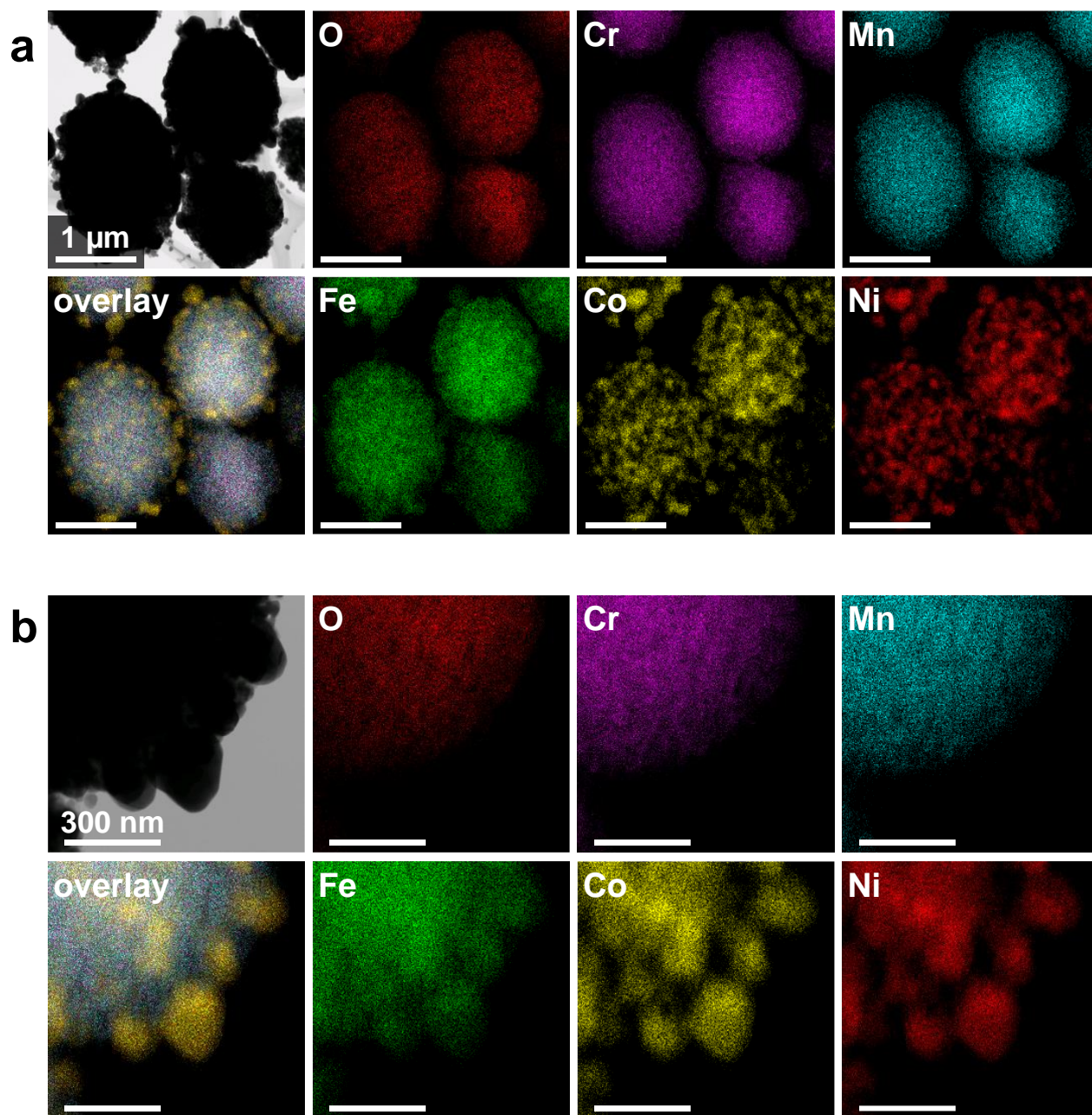


Fig. S7 STEM and EDX mapping images of spent HE-MARIMO. (a) and (b) represent images of different areas.

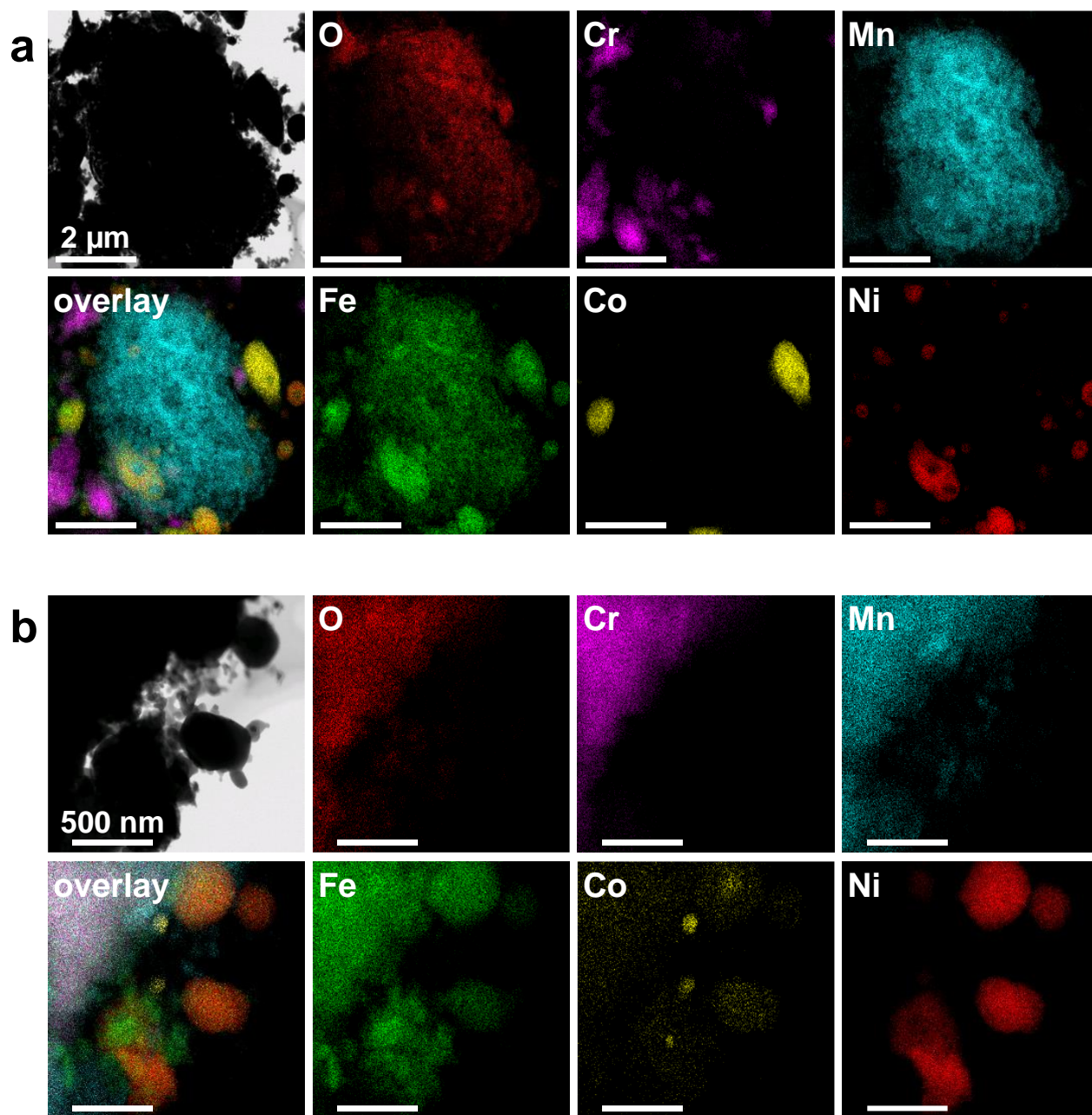


Fig. S8 STEM and EDX mapping images of spent sss-composite. (a) and (b) represent images of different areas.

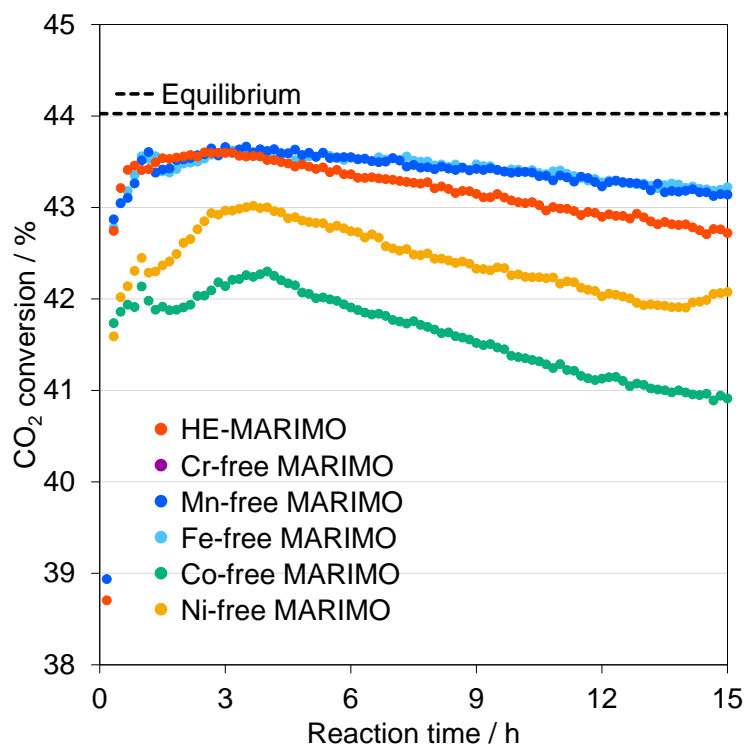


Fig. S9 Enlarged view of CO₂ conversion in RWGS reaction at 700 °C for 15 h.

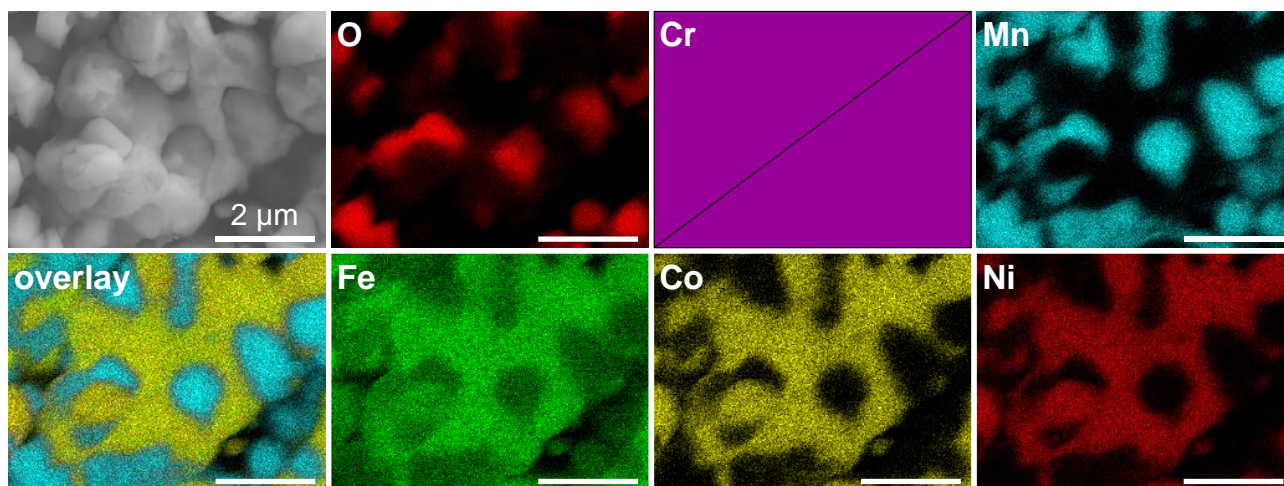


Fig. S10 SEM and EDX mapping images of spent Cr-free MARIMO.

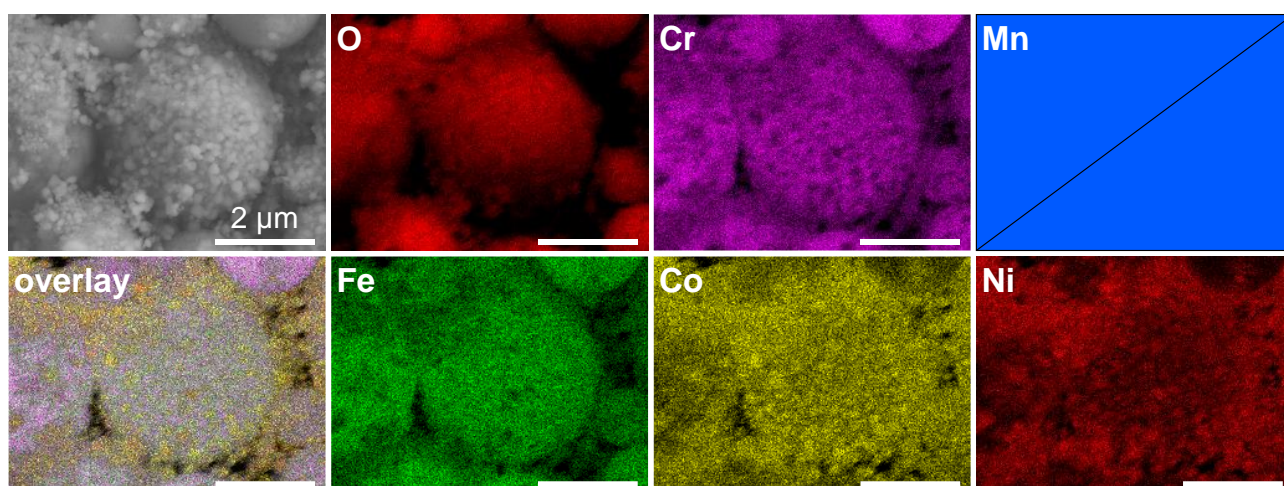


Fig. S11 SEM and EDX mapping images of spent Mn-free MARIMO.

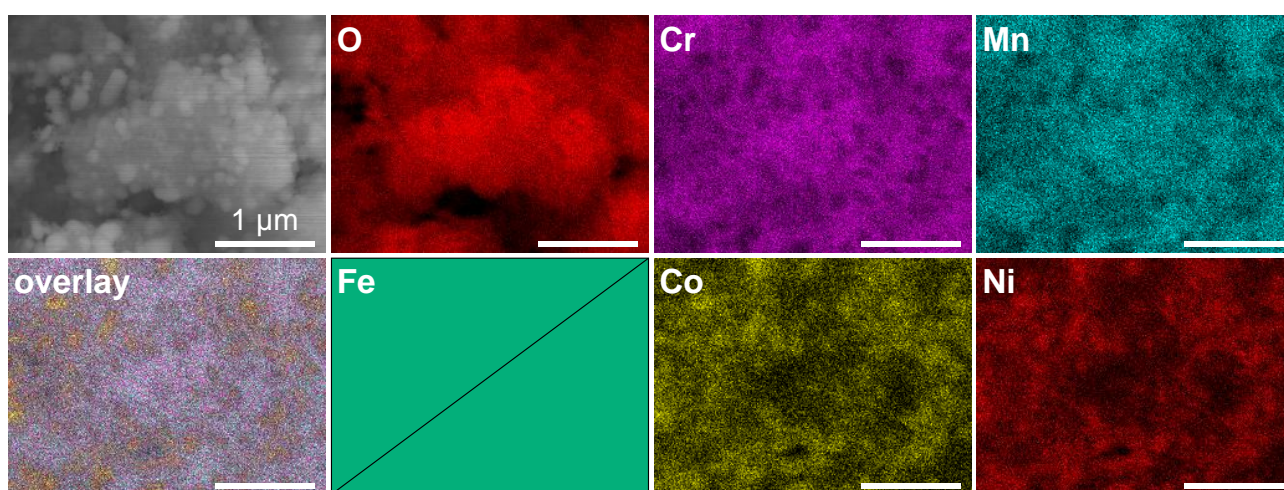


Fig. S12 SEM and EDX mapping images of spent Fe-free MARIMO.

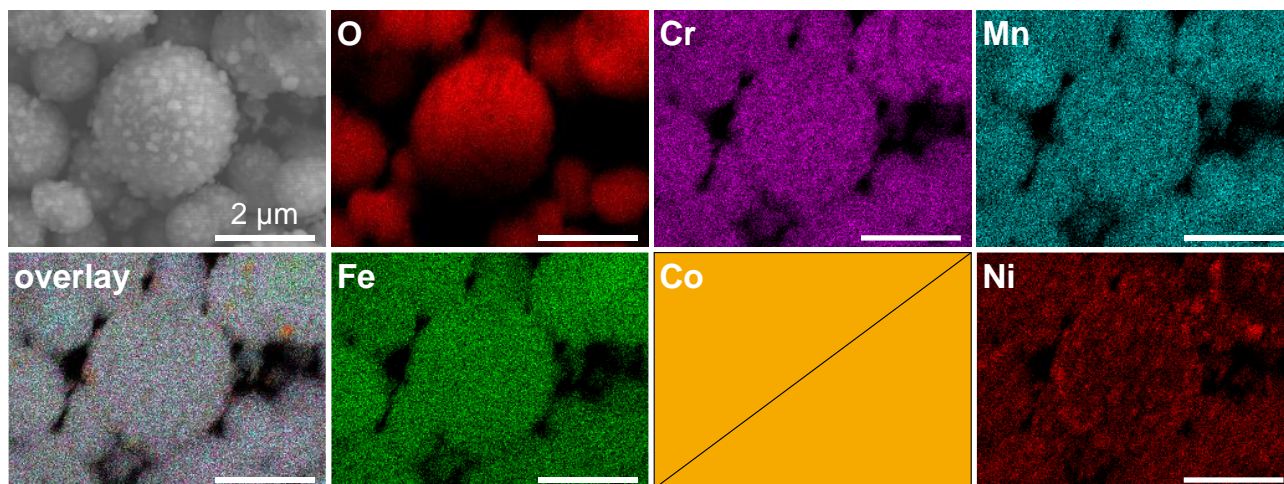


Fig. S13 SEM and EDX mapping images of spent Co-free MARIMO.

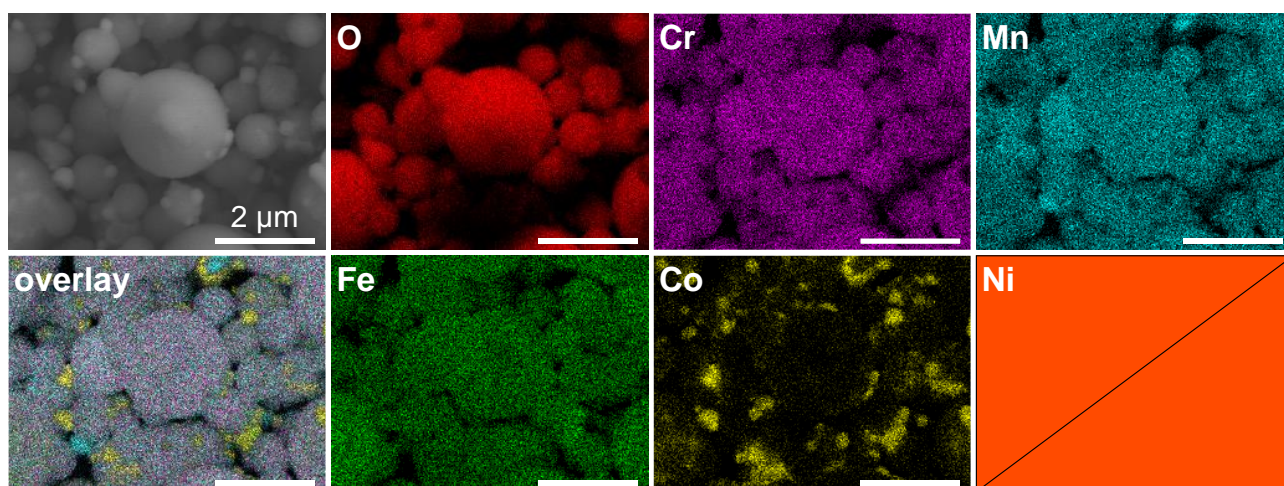


Fig. S14 SEM and EDX mapping images of spent Ni-free MARIMO.

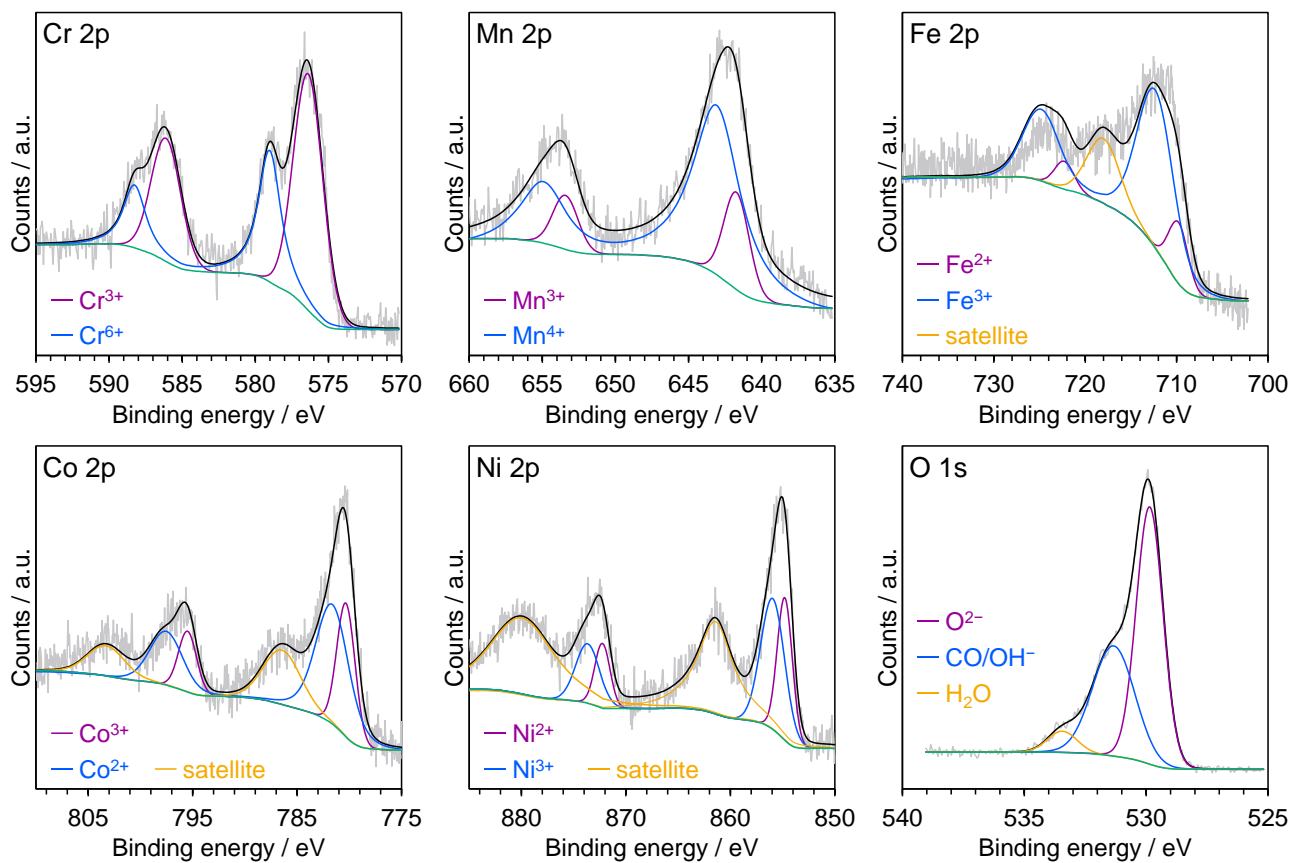


Fig. S15 XPS spectrum of HE-MARIMO before use. Grey, black, and green lines represent original data, simulation, and Shirley background, respectively.

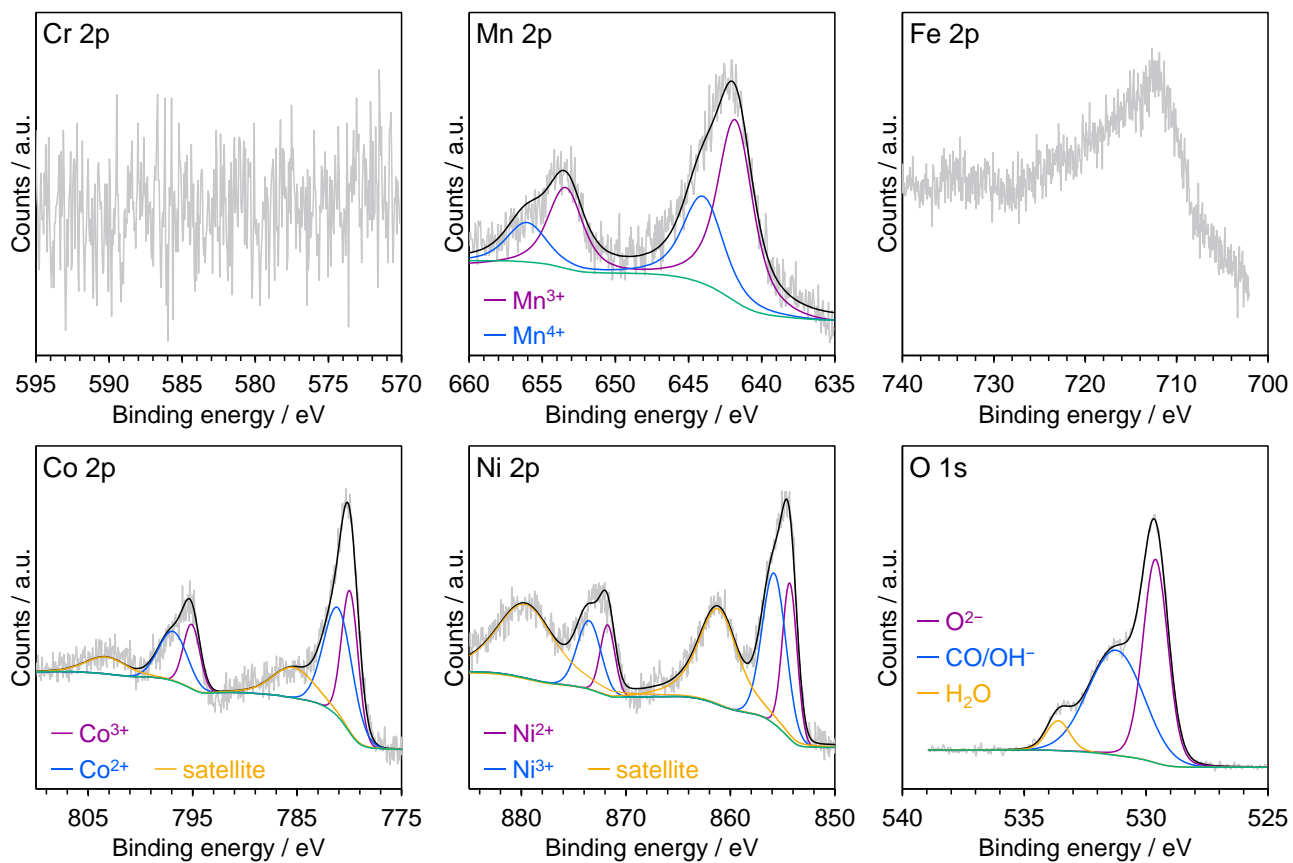


Fig. S16 XPS spectrum of Cr-free MARIMO before use. Grey, black, and green lines represent original data, simulation, and Shirley background, respectively. Curve fitting of Fe 2p spectrum was not performed because the intensity was low and peaks could not recognize well.

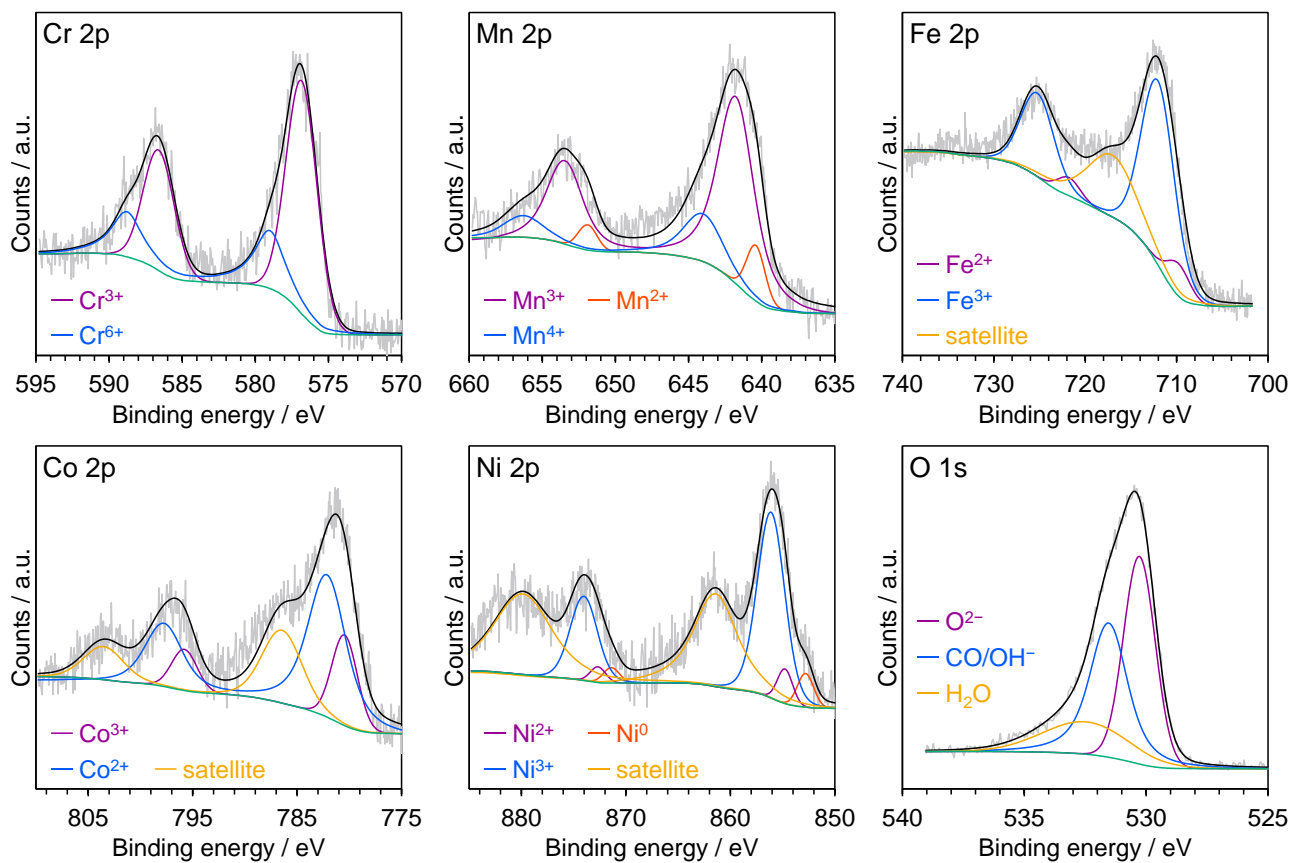


Fig. S17 XPS spectrum of spent HE-MARIMO. Grey, black, and green lines represent original data, simulation, and Shirley background, respectively.

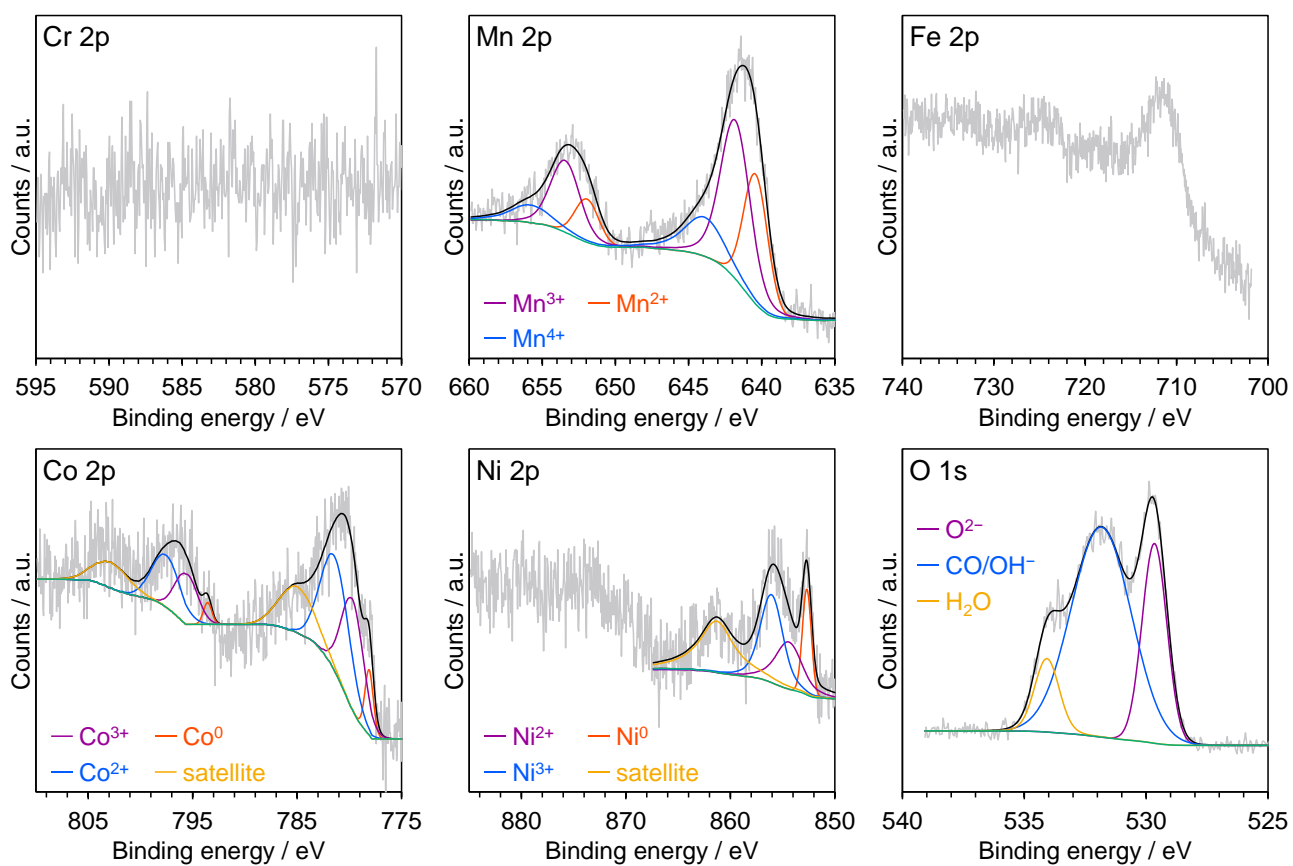


Fig. S18 XPS spectrum of spent Cr-free MARIMO. Grey, black, and green lines represent original data, simulation, and Shirley background, respectively. Curve fitting of Fe 2p spectrum was not performed because the intensity was low and peaks could not recognize well.

Table S1. Solvothermal reaction conditions and yields to obtain HE-MARIMO and quaternary MARIMOs.

Sample	Amount of metal sources in precursor solution / mmol					Yield ^a
	Cr(NO ₃) ₃	Mn(NO ₃) ₂	Fe(NO ₃) ₃	Co(NO ₃) ₂	Ni(NO ₃) ₂	/ %
HE-MARIMO	0.700	0.700	0.700	0.700	0.700	109
Cr-free MARIMO	-	0.875	0.875	0.875	0.875	119
Mn-free MARIMO	0.875	-	0.875	0.875	0.875	139
Fe-free MARIMO	0.875	0.875	-	0.875	0.875	120
Co-free MARIMO	0.875	0.875	0.875	-	0.875	116
Ni-free MARIMO	0.875	0.875	0.875	0.875	-	96

^a Yield was calculated as trimetal tetraoxide (M₃O₄).

Table S2. Elemental ratios and crystal sizes of HE-MARIMO and quaternary MARIMOs.

Sample	Element ratio ^a / at%					Crystallite size ^b / nm
	Cr	Mn	Fe	Co	Ni	
HE-MARIMO	20.6	17.5	22.5	19.0	20.4	6.0
Cr-free MARIMO	-	24.0	26.5	23.9	25.6	5.3
Mn-free MARIMO	24.6	-	25.2	24.1	26.1	7.6
Fe-free MARIMO	26.3	24.1	-	23.2	26.3	5.7
Co-free MARIMO	26.5	20.8	27.9	-	24.7	2.9
Ni-free MARIMO	27.1	20.8	29.6	22.5	-	6.9

^a Element ratio was determined by XRF analysis.

^b Crystallite size of product after calcination at 500 °C for 60 min was estimated by Scherrer's equation.

Table S3. Standard redox potentials of metals.^a

Electrode reaction	E^0 / V
$\text{Cr}^{2+} + 2\text{e}^- \rightleftharpoons \text{Cr}$	-0.90
$\text{Mn}^{2+} + 2\text{e}^- \rightleftharpoons \text{Mn}$	-1.18
$\text{Fe}^{2+} + 2\text{e}^- \rightleftharpoons \text{Fe}$	-0.440
$\text{Co}^{2+} + 2\text{e}^- \rightleftharpoons \text{Co}$	-0.277
$\text{Ni}^{2+} + 2\text{e}^- \rightleftharpoons \text{Ni}$	-0.257

^a A. J. Bard, R. Parsons, J. Jordan, Eds., *Standard Potentials in Aqueous Solution*, Marcel Dekker, New York 1985.

Table S4. Crystal sizes of oxides and metal species in spent HE-MARIMO and spent quaternary MARIMOs.

Sample	Crystallite size ^a / nm	
	Oxides ^b	Metal species ^c
Spent HE-MARIMO	33	51
Spent Cr-free MARIMO	54 ^d	41
Spent Mn-free MARIMO	42	32
Spent Fe-free MARIMO	17	61
Spent Co-free MARIMO	37	43
Spent Ni-free MARIMO	42	61

^a Crystallite sizes of products after the RWGS reaction at 700 °C for 15 h were estimated by Scherrer's equation.

^b Based on a peak of 311 diffraction of spinel oxide around 35°.

^c Based on a peak of 111 diffraction of fcc metal around 44°.

^d Based on a peak of 200 diffraction of rock-salt oxide around 41°.